Behavior of Sandwich Tubular-hat Sections with Aluminum Foam Filler Subjected to Low Velocity Impact Load

Hung Anh Ly* **& Thinh Thai Quang**

Department of Aerospace Engineering, Faculty of Transportation Engineering,
Ho Chi Minh City University of Technology (HCMUT), Ho Chi Minh City, Vietnam
*E-mail: lyhunganh@hcmut.edu.vn

Abstract. In this paper, a comprehensive literature review is presented regarding dynamic progressive buckling analyses of foam-filled hat section columns. The results obtained from a numerical simulation were in good agreement with the theoretical predictions. Remarks and analyses are given about the influence of aluminum foam filling in tubular-hat structures. The contribution of aluminum foam to increase both the crushing load and the mass specific energy absorption is significant. In addition, effects of geometrical parameters like wall thickness are discussed to study the role of thin walls in foam-filled hat sections.

Keywords: *energy absorption; foam-filled; impact; thin-walled; tubular sections.*

1 Introduction – Literature Review

1.1 Crushing Resistance of Non-filled Hat Sections

1.1.1 Top-hat Section

Top-hat structures are divided into 'L' shaped elements as shown in Figure 1 from White, *et al*. [1] in order to study the axial crushing resistance.

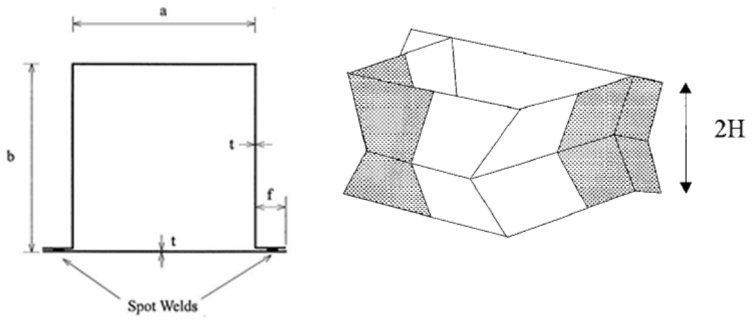

Figure 1 (a) Cross-section geometry of a top-hat column. (b) Four asymmetric elements forming a collapse profile [1].

Received June 22nd, 2016, 1st Revision February 9th, 2017, 2nd Revision April 12th, 2017, Accepted for publication April 27th, 2017.
 ISSN: 2337-5779, DOI: 10.5614/j.eng.technol.sci.2017.49.1.9

With the assumption of a perfectly plastic material, the mean static crushing force (P_m), folding wave length ($2H$) and rolling radius (r) [1] are presented in Eqs. (1) to (3):

$$P_m/M_0 = 32.89(L/t)^{1/3} \tag{1}$$

$$H/t = 0.39(L/t)^{2/3} \tag{2}$$

$$r/t = 0.45(L/t)^{1/3} \tag{3}$$

where t is the thickness of the column, $L = (2a + 2b + 4f)$ and $M_0 = (1/4)\sigma_y t^2$ with σ_y is yield stress.

Regarding the change of the flow stress in the structure, Wierzbicki, *et al.* [2] introduced a simplified approach through a power law approximation for strain hardening materials with $\sigma(\varepsilon)/\sigma_u = (\varepsilon/\varepsilon_u)^n$. The mean static crushing load, folding length and rolling radius of a popular mild steel ($\varepsilon_u = 0.3$, $n = 0.1$), including the variation of the flow stress, are shown in Eqs. (4) to (6) [1]:

$$\bar{P}_m/M_u = 35.55(L/t)^{0.29} \tag{4}$$

$$H/t = 0.478(L/t)^{0.64} \tag{5}$$

$$r/t = 0.563(L/t)^{0.32} \tag{6}$$

With respect to the impact crushing load, the empirical uniaxial constitutive equation of Cowper-Symonds is employed to evaluate material strain rate effects, thereby forming a connection between dynamic crushing force $(\bar{P}_m)^d$ and mean static crushing force $\bar{P}_m$ as expressed in Eq. (7):

$$(\bar{P}_m)^d/\bar{P}_m = 1 + (\dot{\varepsilon}_{av}/D)^{1/p} \tag{7}$$

with the mean strain rate during axial crushing of an asymmetric superfolding element as expressed in Eq. (8) [3]:

$$\dot{\varepsilon}_{av} = tV_m/\left(4\delta_e r_f\right) \tag{8}$$

where $V_m = V/2$ is the mean velocity, V is the impact velocity and $r/r_f = 1.36$, $\delta_e = 0.73H$, and $2\delta_e$ is the final length of a folding wave.

Finally, the mean impact crushing force for a top-hat section with strain hardening and strain rate sensitive according to White, *et al.* [1] is defined in Eq. (9):

$$(\bar{P}_m)^d/\bar{P}_m = 1 + [0.87V/(L^{0.96}t^{0.04}D)]^{1/p} \tag{9}$$

The mean impact crushing force is computed by multiplying the mean static crushing force to strain rate factor. Abramowicz, *et al.* [3] predicted the strain rate for an asymmetric superfolding element under impact axial loading as

$\dot{\varepsilon}_{av} = Vt/(4.3Hr)$. The mean impact crushing force P_c^D is determined with Eq. (10):

$$P_c^D = P_c^S\left[1 + (\dot{\varepsilon}_{av}/D)^{1/p}\right] \tag{10}$$

where P_c^S is the mean static crushing force. H and r are employed by White *et al.* [1] from a theoretical prediction of static crushing to compute the strain rate and the mean impact force.

Wang, *et al*. [4] recognized that not only the mean impact crushing force can be found by the mean static crushing force multiplied with a coefficient relating to the strain rate, but the same procedure can also be applied to static circumstances. Thus, Wang, *et al.* [4] introduced a modification to the prediction of White, *et al.*[1] for top-hat and double-hat sections.

The mean impact crushing force for top-hat structures can be given as in Eq. (11) [4]:

$$\begin{aligned}(\bar{P}_m)^d = \bar{P}_m\left[1 + (\dot{\varepsilon}_{av}/D)^{1/p}\right] = t^2\sigma_0\{&6.08(r/t) + 1.08(L/H) + \\ &3.15(H/r) + [tV/(4.3D)]^{1/p}\left[(6.08/t)H^{-1/p}r^{1-1/p} + \right. \\ &\left.1.08LH^{-1-1/p}r^{-1/p} + 3.15H^{1-1/p}r^{-1-1/p}\right]\}\end{aligned} \tag{11}$$

Where the equivalent flow stress of material σ_0 is defined by Eq. (12) [5]:

$$\sigma_0 = \left\{2\sigma_y\sigma_u^2/[(n+1)^2(n+2)]\right\}^{1/3} \tag{12}$$

In order to get the values of H and r, Eq. (11) is minimized with respect to H and r, which have:

$$\begin{aligned}\partial(\bar{P}_m)^d/\partial H = \\ &-1.08LH^{-2} + 3.15r^{-1} - \\ &(1/p)[tV/(4.3D)]^{1/p}(6.08/t)H^{-1-1/p}r^{1-1/p} - (1 + \\ &1/p)[tV/(4.3D)]^{1/p}1.08LH^{-2-1/p}r^{-1/p} + 3.15(1 - \\ &1/p)[tV/(4.3D)]^{1/p}H^{-1/p}r^{-1-1/p} = 0\end{aligned} \tag{13}$$

$$\begin{aligned}\partial(\bar{P}_m)^d/\partial r = \\ &6.08/t - 3.15Hr^{-2} + \\ &(1 - 1/p)[tV/(4.3D)]^{1/p}(6.08/t)H^{-1/p}r^{-1/p} - \\ &(1/p)[tV/(4.3D)]^{1/p}1.08LH^{-1-1/p}r^{-1-1/p} - (1 + \\ &1/p)\,[tV/(4.3D)]^{1/p}3.15H^{1-1/p}r^{-2-1/p} = 0\end{aligned} \tag{14}$$

From Eqs. (13) and (14), a system of two equations with two unknowns is created. A numerical iteration method is utilized to solve this system and then the mean impact crushing force is gained by substituting the values of H and r into Eq. (11).

1.1.2 Double-hat Section

The double-hat section is analyzed in a similar way to the top-hat section. In the model of White, *et al.* [1], one layer of wrinkles comprises eight superfolding elements, as shown in Figure 2. For a perfectly plastic material, the mean static crushing load is expressed as in Eqs. (15) to (17) [1]:

$$P_m/M_0 = 52.2(L/t)^{1/3} \tag{15}$$

$$H/t = 0.247(L/t)^{2/3} \tag{16}$$

$$r/t = 0.358(L/t)^{1/3} \tag{17}$$

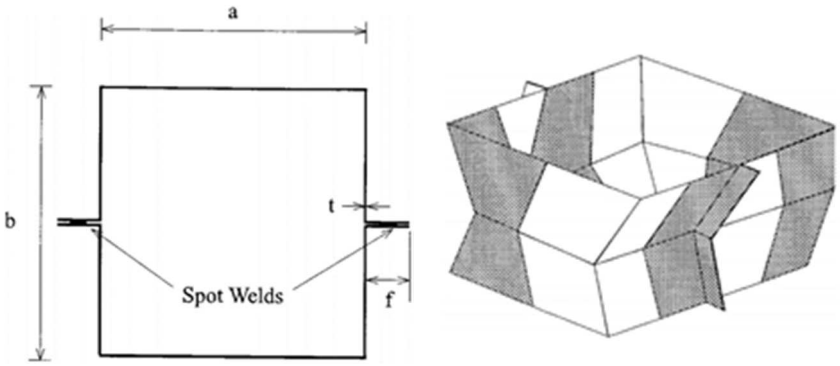

Figure 2 (a) Double-hat column cross-section. (b) Eight asymmetric elements forming a collapse profile [1].

A strain-hardening material ($\varepsilon_u = 0.3,\ n = 0.1$) is taken as an example. The results are expressed in Eqs. (18) to (20) [1]:

$$\bar{P}_m/M_u = 58.15(L/t)^{0.29} \tag{18}$$

$$H/t = 0.532(L/t)^{0.64} \tag{19}$$

$$r/t = 0.45(L/t)^{0.32} \tag{20}$$

In terms of material strain rate effects, the same procedure as used for top-hat structures is utilized to obtain the mean impact axial crushing force of a double-hat structure. Thus in Eq. (21) [1]:

$$(\bar{P}_m)^d/\bar{P}_m = 1 + [0.973V/(L^{0.96}t^{0.04}D)]^{1/p} \tag{21}$$

Wang, *et al*. [4] modified the model of White *et al*. [1] and gave the expression of the mean impact crushing force for the double-hat section with Eq. (22):

$$(\bar{P}_m)^d = \bar{P}_m\left[1 + (\dot{\varepsilon}_{av}/D)^{1/p}\right] = t^2\sigma_0\{12.164(r/t) + 1.08(L/H) + 6.29(H/r) + [tV/(4.3D)]^{1/p}\left[(12.164/t)H^{-1/p}r^{1-1/p} + 1.08LH^{-1-1/p}r^{-1/p} + 6.29H^{1-1/p}r^{-1-1/p}\right]\} \quad (22)$$

and $\partial(\bar{P}_m)^d/\partial H = 0$ along with $\partial(\bar{P}_m)^d/\partial r = 0$ give:

$$\partial(\bar{P}_m)^d/\partial H = -1.08LH^{-2} + 6.29r^{-1} - (1/p)[tV/(4.3D)]^{1/p}(12.164/t)H^{-1-1/p}r^{1-1/p} - (1 + 1/p)[tV/(4.3D)]^{1/p}1.08LH^{-2-1/p}r^{-1/p} + 6.29(1 - 1/p)[tV/(4.3D)]^{1/p}H^{-1/p}r^{-1-1/p} = 0 \quad (23)$$

$$\partial(\bar{P}_m)^d/\partial r = 12.164/t - 6.29Hr^{-2} + (1 - 1/p)[tV/(4.3D)]^{1/p}(12.164/t)H^{-1/p}r^{-1/p} - (1/p)[tV/(4.3D)]^{1/p}1.08LH^{-1-1/p}r^{-1-1/p} - (1 + 1/p)[tV/(4.3D)]^{1/p}6.29H^{1-1/p}r^{-2-1/p} = 0 \quad (24)$$

An iteration method is employed to solve the system of Eqs. (23) and (24) and then substituting into Eq. (22) to get the mean impact axial crushing force.

1.2 Crushing Resistance of Sandwich Hat Sections with Foam-filler

1.2.1 Energy Absorption of Aluminum Foam

Wang, *et al.* [6] conducted a large number of experiments and recognized that the strain rate can be neglected for the aluminum foam if the initial impact velocity is lower than 8 m/s (Hanssen, *et al.* [7] showed that this is also accurate when the initial impact velocity is up to 25 m/s). To obtain the comprehensive crushing characteristic of the aluminum foam, some aluminum foam blocks are compressed in axial direction until an extremely high strain of over 0.85 and a common relationship are obtained, as shown in Figure 3.

According to Figure 3, there are two areas in the stress-strain curve of aluminum foam:

1. The plateau stress, σ_f, is a long stable crushing region with a constant stress.
2. The densification strain, ε_{ep}, is the rise of stress after a specific strain.

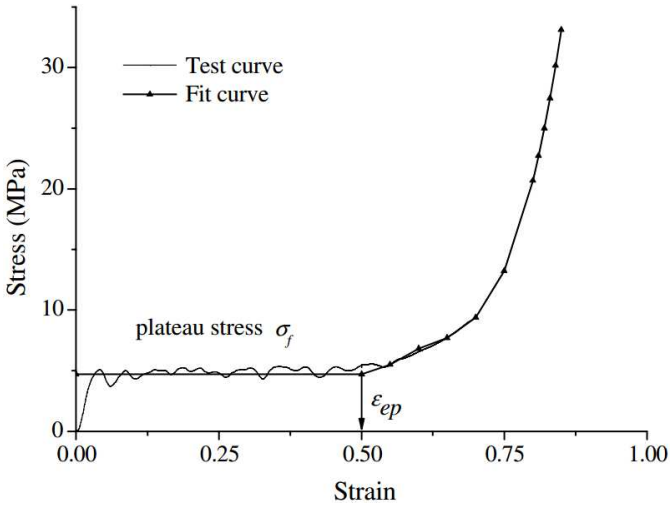

Figure 3 Stress-strain curves of aluminum foam [4].

In order to facilitate the calculation of the theoretical analysis, a polynomial of degree 3 is employed to fit the test data after the ε_{ep} in a least-squares sense. The constitutive relationship of aluminum foam between stress and strain can be written as in Eq. (25):

$$\sigma = \begin{cases} \sigma_f & when\ \varepsilon \le \varepsilon_{ep} \\ \sigma_f(1 + b_3\lambda^3 + b_2\lambda^2 + b_1\lambda) & when\ \varepsilon > \varepsilon_{ep} \end{cases} \tag{25}$$

where $\lambda = \varepsilon - \varepsilon_{ep}$; $b_1, b_2\ and\ b_3$ are the coefficients of the polynomial divided by σ_f.

In accordance with Figure 3, the volume reduction of the aluminum foam filled in the top-hat and double-hat sections with a height of $4H$ is defined by Eq. (26)[4]:

$$\begin{aligned} \Delta V = {} & (0.73H + 0.5t)(0.27 \times 2H + t) \times 2(a + b) + 4ab \times \\ & 0.73H \approx 0.79(a + b)H^2 + 2Ht(a + b) + 4ab \times 0.73H \end{aligned} \tag{26}$$

The total volume strain is defined by Eq. (27).

$$\varepsilon = \Delta V/V = \varepsilon_{ep} + 0.198(a + b)H/(ab) + \beta_0 \tag{27}$$

where $\beta_0 = 0.73 - \varepsilon_{ep} + (a + b)t/2ab$ and $V = 4Hab$ is the original volume of the aluminum foam in the hat sections with a height of $4H$.

As illustrated in the assumptions, the aluminum foam is taken as an isotropic material. The energy absorption of the aluminum foam can be computed with Eq. (28) [4]:

$$E_f^D = \int_0^{\varepsilon_{ep}} 4\sigma_f abHd\varepsilon + \int_{\varepsilon_{ep}}^{\varepsilon} 4\sigma_f(1 + b_3\lambda^3 + b_2\lambda^2 + b_1\lambda)abHd\varepsilon = 4abH\sigma_f(\varepsilon + b_3\lambda^4/4 + b_2\lambda^3/3 + b_1\lambda^2/2) \quad (28)$$

1.2.2 Top-hat section

Wang, *et al.* [4] utilized the coupling method to calculate the total energy absorption of a folding element with foam-filler as follows with Eq. (29):

$$E_{c,f}^D = E_c^D + E_f^D = \sigma_0 t^2 H[24.33(r/t) + 1.37\pi(L/H) + 12.58(H/r)]\left[1 + (\dot{\varepsilon}_{av}/D)^{1/p}\right] + 4abH\sigma_f(\varepsilon + b_3\lambda^4/4 + b_2\lambda^3/3 + b_1\lambda^2/2) \quad (29)$$

The mean impact crushing force is obtained by $P_{c,f}^D = E_{c,f}^D/\delta_e^D$. Hence, the mean impact crushing force of a foam-filled top-hat section is defined by Eq. (30) [4]:

$$P_{c,f}^D = K_0 + K_1H^4 + K_2H^3 + K_3H^2 + K_4H + K_5r + K_6/H + K_7H/r + K_8H^{-1/p}r^{1-1/p} + K_9H^{-1-1/p}r^{-1/p} + K_{10}H^{1-1/p}r^{-1-1/p} \quad (30)$$

where $\lambda = \varepsilon - \varepsilon_{ep} = \lambda_1 H + \beta$. From Eq. (27), it can be deduced that $\lambda_1 = [0.198(a+b)H]/(ab)$, $\beta = \beta_0$.

The coefficients for the top-hat section are expressed in Eqs. (31) to (41) [4]:

$$K_0 = ab\sigma_f(1 + 0.342b_3\beta^4 + 0.457b_2\beta^3 + 0.685b_1\beta^2) \quad (31)$$

$$K_1 = 0.342ab\sigma_f b_3\lambda_1^4 \quad (32)$$

$$K_2 = ab\sigma_f\lambda_1^3(1.368b_3\beta + 0.457b_2) \quad (33)$$

$$K_3 = ab\sigma_f\lambda_1^2(2.052b_3\beta^2 + 1.371b_2\beta + 0.685b_1) \quad (34)$$

$$K_4 = 1.37ab\sigma_f\lambda_1(1 + b_3\beta^3 + b_2\beta^2 + b_1\beta) \quad (35)$$

$$K_5 = 6.08k\sigma_f t \quad (36)$$

$$K_6 = 1.08Lt^2k\sigma_f \quad (37)$$

$$K_7 = 3.15t^2k\sigma_f \quad (38)$$

$$K_8 = 6.08k\sigma_f t[tv_i/(4.3D)]^{1/p} \quad (39)$$

$$K_9 = 1.08k\sigma_f[tv_i/(4.3D)]^{1/p}Lt^2 \quad (40)$$

$$K_{10} = 3.15k\sigma_f[tv_i/(4.3D)]^{1/p}t^2 \quad (41)$$

where $k = \sigma_0/\sigma_f$

The mean impact crushing force is obtained by minimizing Eq. (30) with respect to H and r, which ultimately results in [4]:

$$K_5 - K_7 H r^{-2} + (1 - 1/p)K_8 H^{-1/p} r^{-1/p} - (1/p)K_9 H^{-1-1/p} r^{-1-1/p} - (1 + 1/p)K_{10} H^{1-1/p} r^{-2-1/p} = 0 \quad (42)$$

$$4K_1 H^3 + 3K_2 H^2 + 2K_3 H + K_4 - K_6 H^{-2} + K_7 r^{-1} - (1/p)K_8 H^{-1-1/p} r^{1-1/p} - (1 + 1/p)K_9 H^{-2-1/p} r^{-1/p} + (1 - 1/p)K_{10} H^{-1/p} r^{-1-1/p} = 0 \quad (43)$$

A system of two equations with two unknowns is constructed from Eqs. (42) and (43). A numerical iteration method is exploited to find out the value of H and r, and subsequently, the mean dynamic crushing force is gained by substituting the values of H and r into Eq. (30).

1.2.3 Double-hat section

The same procedure can be used for the double-hat section. The total energy absorption of the foam-filled superfolding element with an original height of $4H$ is defined by Eq. (44):

$$E_{c,f}^{D} = \sigma_0 t^2 H\left(2 \times 24.33(r/t) + 1.37\pi(L/H) + 2 \times 12.58(H/r)\right)\left[1 + (\dot{\varepsilon}_{av}/D)^{1/p}\right] + 4abH\sigma_f(\varepsilon + b_3\lambda^4/4 + b_2\lambda^3/3 + b_1\lambda^2/2) \quad (44)$$

The mean impact crushing force of a sandwich foam-filled double-hat structure is calculated by Eqs. (30), (42) and (43) with coefficients K_5, K_7, K_8, and K_{10} doubled [4].

1.2.4 Interaction Effect

In order to study the interaction effect of a column with aluminum foam filler such as sandwich top-hat and double-hat sections with foam-filler subjected to axial compressed force, two common methods are exploited [8], namely an 'additive method' and a 'coupling method'.

According to the additive method, the mean crushing force of the foam-filled structure, $P_{m,f}$, is separated into certain additive parts. Each of the parts represents the mean crushing load of every separate component in axial compression. The interaction effect is defined by Eq. (45) [8]:

$$P_{m,f} = \sum P_{m,i} + P_{m,int} \quad (45)$$

where $P_{m,i}$ are the mean crushing loads of each separate component when they are compressed axially, and $P_{m,int}$ is the contribution to $P_{m,f}$ originating from interaction effects. In fact, it is important to the additive method that the interaction effect is excluded from each separate component.

Considering a foam-filled square tube with a cross-section $b \times b$, Santosa, *et al.* [9] suggested a prediction of the mean crushing load:

$$P_{m,f} = P_{m,0} + 2b^2\sigma_f \tag{46}$$

where $P_{m,0}$ is the mean crushing load of empty hat structures. In Eq. (46), the contribution of the interaction effects resembles the mean crushing load of a free foam column.

Based on a large number of experiments, Hanssen, *et al*. [10] formulated the following empirical formula:

$$P_{m,f} = P_{m,0} + b^2\sigma_f + 5bt\sqrt{\sigma_f\sigma_0} \tag{47}$$

where σ_0 is the flow stress of the material. The interaction effects between the thin wall and the aluminum foam are a function of both geometrical parameters and material.

The mean crushing load of a foam-filled structure is the sum of each separate member as expressed in Eq. (48):

$$P_{m,f} = \sum P_{m,i}^{c} \tag{48}$$

where $P_{m,i}^{c}$ are the contributions to $P_{m,f}$ from each member. There is a change in the folding wavelength and the effective crushing distance when aluminum foam filler is used.

A typical investigation of the coupling method is the research by Abramowicz, *et al.* [11] on the mean crushing load of polyurethane foam-filled columns. To identify the interaction effects of each member and the energy absorption effectively, the coupling method was utilized in the present study.

Many researchers designate $\sigma_f A$ as the uniaxial crushing resistance of aluminum foam. However, this practice is only suitable and reasonable when the aluminum foam is pressed until approximately 50%. In fact, it is important to notice that the ultimate strain of aluminum foam is higher than 0.73 (given that the effective impact crushing distance is regarded as 0.73 of the initial superfolding element's length). From Figure 3, there is a boom of stress in the aluminum foam compression after a long stable duration. The energy absorption in this area is considerable and should be included. The column also has some

contribution to the interaction effect because H and r are changed in the sandwich structure with aluminum foam filling.

The interaction effect originating from the column and the aluminum foam is expressed in Eqs. (49) to (51):

$$P_{int} = P_{c,f} - P_c - ab\sigma_f \tag{49}$$

$$P_{int,c} = P_c' - P_c \tag{50}$$

$$P_{int,f} = P_{int} - P_{int,c} \tag{51}$$

where P_c' is the load of the column based on the length of the superfolding element of the foam-filled sections.

2 Numerical Simulation

2.1 Model Geometry

Figure 4 illustrates the simulated model in LS-DYNA. The detailed notation of cross-section parameters is presented in Figure 1(a) for top-hat sections and Figure 2(a) for double-hat sections.

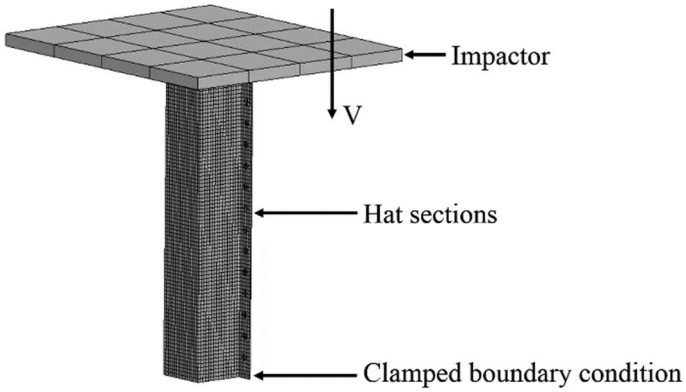

Figure 4 Geometrical model of hat-section specimens in numerical simulation.

Tables 1 and 2 give geometrical parameters of top-hat and double-hat sections, respectively (two tubes for each of case).

Table 1 Geometry of Top-hat sections and initial velocity of the impactor.

Tube	a (mm)	b (mm)	L (mm)	t (mm)	f (mm)	V (m/s)
TH1	48.75	52.5	250	2.98	36.5	8
TH2	50	50	260	1.1	15	8

Table 2 Geometry of Double-hat sections and initial velocity of the impactor.

Tube	a (mm)	b (mm)	L (mm)	t (mm)	f (mm)	V (m/s)
DH1	40	40	210	1	10	8
DH2	50	50	200	1.1	15	8

2.2 Mesh Size

Belytschko-Tsay shell elements are employed to simulate the wall of the hat sections. The size of the shell elements is chosen with a suitable ratio of shell element length to hat-section perimeter. In this study, it was lower than 0.015.

The default eight-node solid element is used to model the rigid impactor. In this study, the foam block was simulated as a solid element with a ratio of solid element side to hat-section perimeter below 0.02.

2.3 Boundary and Contact Conditions

The bottom of the tube is clamped; the other end of the tube, which is struck by an impactor with an initial velocity of 8 m/s, is free.

Automatic-node-to-surface contact is applied for the contact between the impactor and the hat-structures. In order to avoid interpenetration of folds generated during axial collapse of the structure, automatic-single-surface contact is used. The contacts between the impactor and the foam filler, the column walls and foam filler are automatic-surface-to-surface contacts.

2.4 Constitutive Modeling of Material

2.4.1 Material of Thin Wall

The piecewise linear plasticity algorithm was applied for the material of the hat-structures. The hat-structures were made of mild steel RSt37 [5],[12] with mechanical properties as shown in Table 3. Where ρ is density, E is Young's modulus, σ_0 is initial yield stress, σ_u is ultimate stress, ν is Poisson's ratio, n is the power law exponent, D and q are the coefficients of Cowper and Symonds's equation.

Table 3 Mechanical properties of mild steel RSt37 [5],[12].

ρ (kg/m^3)	E (GPa)	σ_0 (MPa)	σ_u (MPa)	ν	n	D (s^{-1})	q
7830	200	251	339	0.3	0.12	6844	3.91

2.4.2 Aluminum Foam Filler

The accurate and simple model utilized in the simulation was MAT 154 Deshpande-Fleck Foam. Three densities of aluminum foam (0.17, 0.34 and 0.51 g/cm^3) were investigated with parameters as detailed in Table 4.

Table 4 Parameters of aluminum foam [13].

ρ_f (g/cm^3)	E (MPa)	α	γ (MPa)	ε_D	α_2 (MPa)	β	σ_p (MPa)
0.17	337	2.12	1.87	2.77	93.5	5.79	1.15
0.34	1516	2.12	3.92	2.07	60.2	4.39	5.76
0.51	5562	2.12	5.37	1.67	66.9	2.99	14.82

3 Results and Discussions

3.1 Aluminum Foam

Aluminum foam cubes with dimensions of 70 x 70 x 70 mm^3 were used in the compression simulations to compare their compressive behavior obtained from the analyses and experimental results in [13]. From Figure 5, it can be inferred that the difference between the results from the simulation and experimental tests in [13] was insignificant. Hence, the model of aluminum foam in the simulation was suitable and reasonable. As introduced in Section 1.2.1, the curves of three different aluminum foam materials (in Figure 5) were fitted to a polynomial of degree 3 after the ε_{ep} in a least square sense. The results are expressed in Eqs. (52) to (54):

1. Foam 0.17g/cm^3

$$\sigma = \begin{cases} \sigma_f & when\ \varepsilon \le \varepsilon_{ep} = 0.65 \\ \sigma_f(1 + 2258.2\lambda^3 - 512.67\lambda^2 + 39.98\lambda) & when\ \varepsilon > \varepsilon_{ep} = 0.65 \end{cases} \quad (52)$$

2. Foam 0.34g/cm^3

$$\sigma = \begin{cases} \sigma_f & when\ \varepsilon \le \varepsilon_{ep} = 0.5 \\ \sigma_f(1 + 400.34\lambda^3 - 121.78\lambda^2 + 12.68\lambda) & when\ \varepsilon > \varepsilon_{ep} = 0.5 \end{cases} \quad (53)$$

3. Foam 0.51g/cm^3

$$\sigma = \begin{cases} \sigma_f & when\ \varepsilon \le \varepsilon_{ep} = 0.4 \\ \sigma_f(1 + 182.69\lambda^3 - 59.85\lambda^2 + 8.00\lambda) & when\ \varepsilon > \varepsilon_{ep} = 0.4 \end{cases} \quad (54)$$

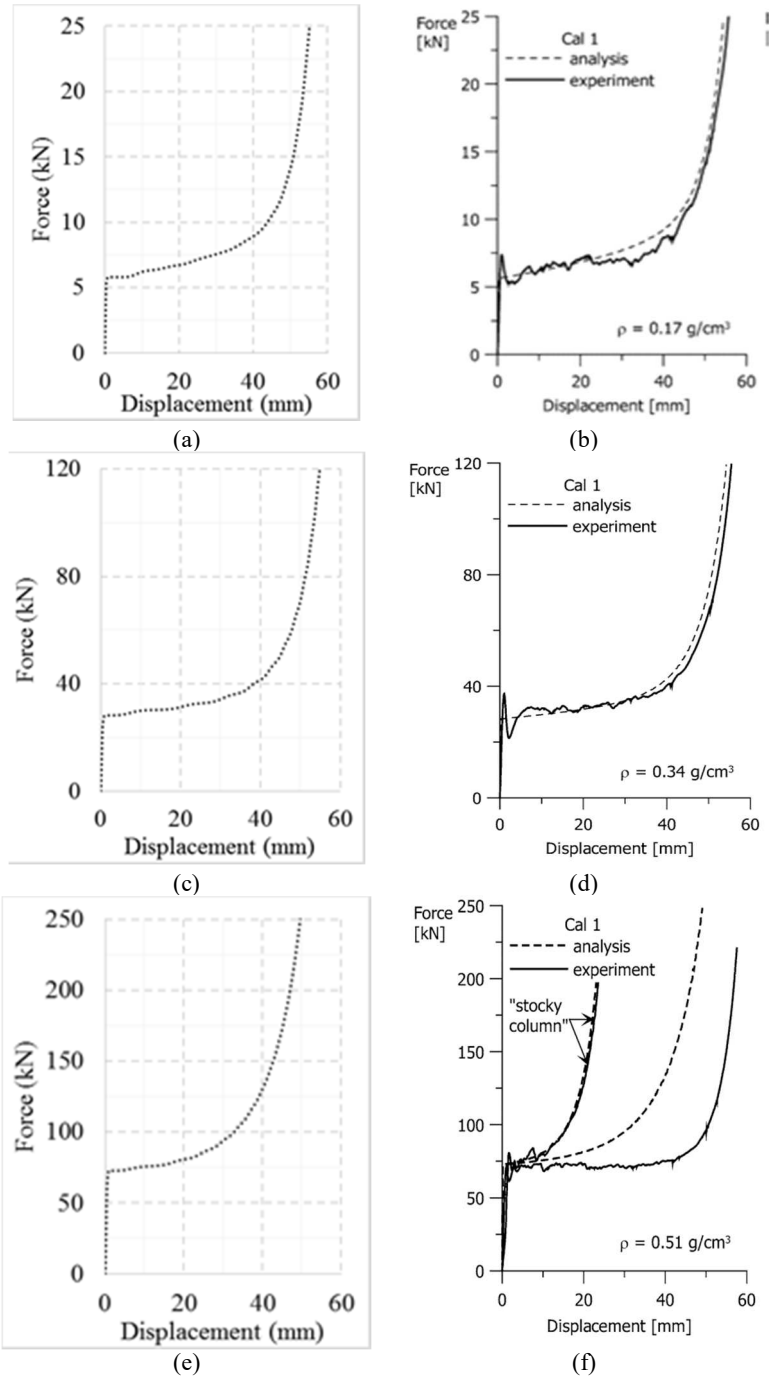

Figure 5 Validation of aluminum foam models. (a), (c) and (e) Results from simulation. (b), (d) and (f) Results from [13].

3.2 Mean Dynamic Axial Crushing Load

A comparison between the theoretical prediction and the numerical analysis of hat-sections filled with three different amounts of aluminum foam is shown in Table 5. It can be inferred that the discrepancy is generally small, acceptable (lower than 10%), except for sections with aluminum foam of 0.51 g/cm^3 (11.59% for TH2 and 14.35% for DH2). The reason can be the fracture of high-density aluminum foam [13] and the dynamic effect not being eliminated completely from simulation. Therefore, the simulation model is valid.

Table 5 Comparison of the mean impact crushing load of hat sections.

Tube	Empty hat			Filled hat			
	Theoretical prediction (kN)	Numerical analysis (kN)	Error (%)	Foam (g/cm^3)	Theoretical prediction (kN)	Numerical analysis (kN)	Error (%)
TH1	123.71	123.31	0.33	0.17	128.96	128.51	0.34
				0.34	147.21	153.71	4.42
				0.51	196.17	195.28	0.46
TH2	21.62	21.73	0.47	0.17	26.36	28.80	9.25
				0.34	41.92	45.10	7.58
				0.51	82.02	72.51	11.59
DH1	28.29	25.88	8.51	0.17	31.33	30.83	1.61
				0.34	41.29	43.26	4.75
				0.51	67.06	60.55	9.70
DH2	35.63	34.38	3.50	0.17	40.36	37.96	5.96
				0.34	55.83	51.90	7.04
				0.51	95.66	81.93	14.35

3.3 Energy Absorption and Interaction Effect

The effect of each component on the interaction effect is presented in Table 6. Eqs. (49)-(51) are used to quantify these results. When filling with aluminum foam, the crushing force of tubular-hat structures and foam-filled components together are higher than of both separately. In the interaction effect, the contribution of the foam filler is dominant, i.e. it far outstrips that of the hat section. Another remark is that the higher the density of the aluminum foam, the bigger the interaction effect becomes.

In order to facilitate the understanding of the relationship with the interaction effect as shown in explicit results in Table 6, a vivid illustration is given in Figure 6 (using the top-hat structure as an example) where these modes represent the mean crushing load or energy absorbing capability. The following conclusions are certain:

$$(a) = (b) + (c);\ (b) > (d);\ (c) > (e);\ (a) > (d) + (e);\ (c) - (e) > (b) - (d)$$

Table 6 Effect of each component on energy absorbing capability.

Individuals			Foam-filled components			Interaction effect			
Empty hat (kN)	Free foam (kN)	Sum (kN)	Foam (g/cm^3)	Hat section component (kN)	Foam filler component (kN)	Total (kN)	Increase in hat section (%)	Increase in foam filler (%)	Total increase (%)
					TH1				
	2.9	126.7	0.17	124.7	4.2	129.0	0.8	43.7	1.8
123.7	14.7	138.5	0.34	125.2	22.0	147.2	1.2	49.0	6.3
	37.9	161.6	0.51	132.7	63.5	196.2	7.2	67.4	21.4
					TH2				
	2.9	24.5	0.17	22.5	3.8	26.4	4.1	33.8	7.6
21.6	14.4	36.0	0.34	22.5	19.4	41.9	4.1	34.7	16.4
	37.1	58.7	0.51	23.2	58.8	82.0	7.3	58.8	39.8
					DH1				
	1.8	30.1	0.17	28.9	2.5	31.3	2.0	34.7	4.0
28.3	9.2	37.5	0.34	28.9	12.4	41.3	2.0	35.0	10.1
	23.7	52.0	0.51	30.3	36.7	67.1	7.2	54.8	29.0
					DH2				
	2.9	38.5	0.17	36.3	4.0	40.4	0.7/2.0	39.9	4.8
35.6	14.4	50.0	0.34	36.3	19.5	55.8	0.7/2.0	35.3	11.6
	37.1	72.7	0.51	38.2	57.4	95.7	2.6/7.3	55.1	31.6

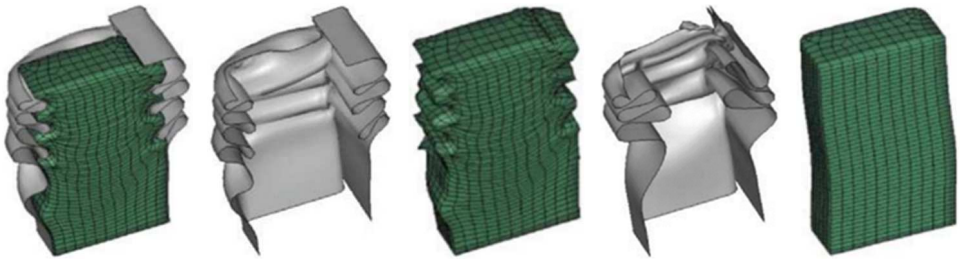

(a) (b) (c) (d) (e)

Figure 6 Simulation of collapse mode expressing the interaction effect [8]. (a) Sandwich top-hat foam-filler. (b) Top-hat component. (c) Foam filler component. (d) Empty top-hat. (e) Free foam column.

3.4 Mass Specific Energy Absorption

The higher the density of the aluminum foam filler, the larger the mean dynamic axial crushing load gets, as already mentioned in Section 3.2. Yet, this remark provides only a superficial conclusion. To quantify the energy-absorbing efficiency of a structure, the mass specific energy absorption (mass SEA) is used as a popular measurement. This is the energy-absorption capacity per unit mass.

This formula is exploited to compute the SEA of the empty and foam-filled tubular-hat structures. The calculation results are presented in Table 7:

Table 7 SEA for empty and foam-filled tubular-hat structures.

	Foam (g/cm^3)	Mass (kg)	Energy (kJ)	SEA (kJ/kg)	Improved (%)
TH1	---	2.05	14.60	7.11	---
	0.17	2.16	15.43	7.16	0.71
	0.34	2.26	18.58	8.23	15.76
	0.51	2.36	23.50	9.95	40.09
TH2	---	0.59	2.83	4.81	---
	0.17	0.70	3.75	5.38	11.88
	0.34	0.80	5.87	7.30	51.70
	0.51	0.91	9.44	10.35	115.06
DH1	---	0.33	2.29	6.87	---
	0.17	0.39	2.87	7.37	7.20
	0.34	0.44	3.98	8.96	30.36
	0.51	0.50	5.44	10.87	58.15
DH2	---	0.45	2.99	6.62	---
	0.17	0.54	3.69	6.90	4.20
	0.34	0.62	4.66	7.54	14.00
	0.51	0.70	7.18	10.23	54.57

Table 7 illustrates the connection between the SEA and the density of the aluminum foam filler. Obviously, the SEA of the aluminum foam-filled tubular-hat structures is higher than that of the empty ones. The higher the density of the aluminum foam filler, the higher the SEA obtained. This means that the structure becomes lighter when it is filled it with aluminum foam to absorb a specific amount of energy. The higher the density of the aluminum foam, the less mass is required. Furthermore, the aluminum foam filling enhances the stability of the structure.

The investigation of the SEA vs. various wall thicknesses for tubes with a cross-section similar to DH1's is shown Figure 7. Generally, the dependence of SEA vs. wall thickness is a linear function with a positive gradient, as indicated in Figure 7. This means that the SEA becomes higher with the increase of column thickness.

Based on Figures 7(a) and (b), the energy absorption capability of double-hat sections is better than that of top-hat sections because the SEA of the former is higher than that of the latter. This is valid for both non-filled and foam-filled cases.

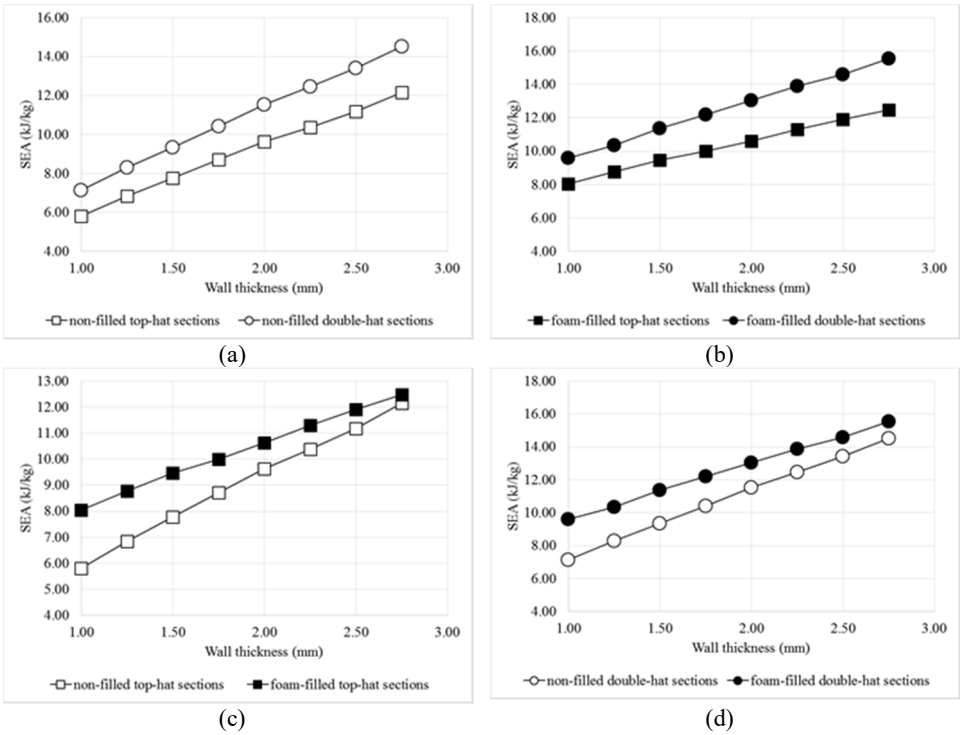

Figure 7 Relationships between SEA and wall thickness of hat sections.

The cause for this outstanding performance is that there are eight superfolding elements in a wrinkle of double-hat sections, whereas top-hat sections have four superfolding elements. The change of the SEA for double-hat sections is faster than that for top-hat ones when raising the column thickness.

In addition, the filling aluminum foam entails a higher SEA and the SEA of the non-filled sections increases faster than that of the foam-filled ones (Figures 7(c) and 7(d)). With a high wall thickness value, the gap between non-filled and foam-filled is bridged. This indicates that the energy absorption primarily comes from the column wall with respect to the thick wall structure.

4 Conclusions

In this study, the behavior of sandwich tubular-hat sections with aluminum foam filler subjected to low velocity impact load was analyzed. The theoretical prediction of the behavior of the aluminum tubular-hat foam-filler structures agreed well with the numerical simulations. The energy absorption capability of double-hat sections is better than that of top-hat sections due to the higher number of superfolding elements. The mean crushing force of tubular-hat

structures and foam filler components together is higher than of both separately. The higher the density of the aluminum foam filler, the more improvement is obtained. Aluminum foam filler has a dominant role in the interaction effect due to its stress-strain property. Meanwhile, the mean crushing force of the column itself rises marginally due to the variation of H and r when using aluminum foam filler. The SEA of the aluminum foam-filler tubular-hat structures is improved in comparison with that of the corresponding non-filled hat sections with the same thickness. For the thick wall structure, the gap between non-filled and foam-filled is narrowed due to the primary influence of the column wall on the energy absorption performance.

References

[1] White, M. & Jones, N., *A Theoretical Analysis for the Dynamic Axial Crushing of Top-hat and Double-hat Thin-walled Sections*, in Proceedings of the Institution of Mechanical Engineers, pp. 307-325, 1999.

[2] Wierzbicki, T. & Abramowicz, W., *Manual of Crashworthiness Engineering*, Cambridge, MA: MIT, 1987.

[3] Abramowicz, W. & Wierzbicki, T., *Axial Crushing of Multicorner Sheet Metal Columns,* Journal of Applied Mechanics, **56**(1), pp. 113-120, Mar. 1989.

[4] Wang, Q., Fan, Z. & Gui, L., *A Theoretical Analysis for the Dynamic Axial Crushing Behaviour of Aluminium Foam-filled Hat Sections,* International Journal of Solids and Structures, **43**(7-8), pp. 2064-2075, 2006.

[5] Ly, H. A., *Behavior of Thin-walled Prismatic Structures Subjected to Low Velocity Impact Loading*, M.A. Thesis, Institut Teknologi Bandung, Indonesia 2007.

[6] Wang, Q., Fan, Z., Gui, L., Wang, Z. & Fu, Z., *Experimental Studies on the Axial Crash Behavior of Aluminum Foam-filled Hat Sections*, in *Frontiers of Mechanical Engineering in China*, Dec. 2006.

[7] Hanssen, A.G., Langseth, M. & Hopperstad, O.S., *Static and Dynamic Crushing of Square Aluminium Extrusions with Aluminum Foam Filler,* International Journal of Impact Engineering, **24**(4), pp. 347-383, Apr. 2000.

[8] Song, H., Fan, Z., Yu, G., Wang, Q. & Tobota, A., *Partition Energy Absorption of Axially Crushed Aluminum Foam-filled Hat Sections,* International Journal of Solids and Structures, **42**(9-10), pp. 2575-2600, May 2005.

[9] Santosa, S. & Wierzbicki, T., *Crash Behavior of Box Columns Filled with Aluminum Honeycomb or Foam,* Computers & Structures, **68**(4), pp. 343-367, Aug. 1998.

[10] Hanssen, A.G., Langseth, M. & Hopperstad, O.S., *Static Crushing of Square Aluminium Extrusions with Aluminium Foam Filler,* International Journal of Mechanical Sciences, **41**(8), pp. 967-993, Aug. 1999.

[11] Abramowicz, W. & Wierzbicki, T., *Axial Crushing of Foam-filled Columns,* International Journal of Mechanical Sciences, **30**(3-4), pp. 263-271, 1988.

[12] Santosa, S.P., Wierzbicki, T., Hanssen, A.G. & Langseth, M., *Experimental and Numerical Studies of Foam-filled Sections,* International Journal of Impact Engineering, **24**(5), pp. 509-534, May 2000.

[13] Reyes, A., Hopperstad, O.S., Berstad, T.A., Hanssen, G. & Langseth, M., *Constitutive Modeling of Aluminum Foam including Fracture and Statistical Variation of Density,* European Journal of Mechanics – A/Solids, **22**(6), pp. 815-835, 2003.